# RSC Advances

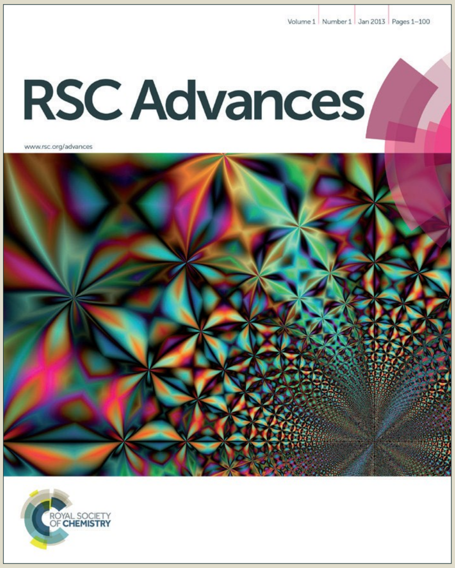

ROYAL SOCIETY OF CHEMISTRY

www.rsc.org/advances

# Theoretical study on complexation of U(VI) with ODA, IDA and TDA based on density functional theory

Yiming Ren,[a] Hao Tang,[a] Lang Shao,[a] Jingrong Zhong,[a] Mingfu Chu,[a] Ruizhu Yang*[a] and Chuipeng Kong**[b]

[a]*Institute of Materials, China Academy of Engineering Physics, Mianyang, China*

[b]*State Key Laboratory of Theoretical and Computational Chemistry, Institute of Theoretical Chemistry, Jilin University, Changchun, China, 130023*

Emails of corresponding authors:

Ruizhu Yang: yangruizhu@caep.cn

Chuipeng Kong: kongerer@jlu.edu.cn

## Abstract

This study aims to understand the complexation of U(VI) with oxydiacetic acid (ODA), iminodiacetic acid (IDA) and thiodiacetic acid (TDA) through density functional theory (DFT) calculations. The structures, complexation stabilities and bonding nature were investigated for U(VI)/XDA complexes (XDA is short for the three ligands). The calculations have proved that tridentate structure is more favorable than terminal bidentate ones for all stoichiometries, and steric hindrance is a factor that cannot be ignored especially for 1:2 complexes. The binding stabilities of the ligands and relative binding groups are in the sequences of IDA > ODA >> TDA and C=O > $OH^-$ >> $H_2O$ > X ($O_{ether}$, N and S), respectively. All of the coordination bonds exhibit typical iconicity. The coordination bonds are mainly contributed by the interactions of U 5f-orbital and O(=C)/X p-orbitals. The strength of all coordination bonds follows the order U-O(=C) > U-N > U-O($H_2$) ≈ U-$O_{ether}$ > U-S. U-S interaction was solidly confirmed by MO and AIM analysis, which is found for U(VI)/TDA complexes for the first time. U-X bonds play an important role in U(VI)/XDA coordination.

Keywords: uranyl, DFT, ODA, IDA, TDA

# 1. Introduction

The coordination chemistry of actinides is of great importance, not only for the development of new extractants for the separation of actinides from irradiated nuclear fuel, but also for the technology concerning the storage of highly radioactive waste materials. Also, to study the complexation of actinides and ligands is of great significance for the prediction of migration behavior of these radioactive elements in the geosphere[1]. In comparison to traditional organo-phosphorous extractants (such as TBP, TRPO, etc.), carboxyl substitutes are more widely studied and applied because the radiation degradation products are less detrimental to the separation processes. In addition, on the issues of environmental protection and human health, the carboxyl extractants which only consist of C/O/H and sometimes N elements can be completely incinerated, therefore, the amount of secondary waste released from nuclear industries is largely reduced.

Numerous studies have shown that carboxyl complexant have excellent performances on actinide coordination, such as gluconate[2], dipicolinamide[3], terephthalic acid[4], etc. Bifunctional chelating ligands have attracted great concerns among these carboxyl extractants (DMOGA, TMOGA[5, 6], etc.), due to strong binding ability towards actinides and good organic solubility. As is representative for these chelating ligands, ODA as well as its derivatives has been concerned a lot[7] (molecular structure as seen in Fig. 1). Most of these studies were focused on complexation of U(VI) with ODA and its derivatives. Studies have shown a strong affinity between U(VI) and ODA. Friese et al.[8] compared the complexation rate and stability of ODA complexes with Np(V) and U(VI), and found that the rate of formation of the respective 1:1 complexes was faster for Np(V) than U(VI), but a stronger thermodynamic driving force for the latter. Rao et al.[9] found three U(VI)/ODA complexes ($UO_2L$, $UO_2L_2$ and $UO_2HL_2$) using potentiometry and calorimetry, and pointed out that in the 1:2 $UO_2L_2$ complex, the second ODA ligand could be bidentate or in a dynamic mode between tridentate and bidentate coordination configurations, and $UL_2HL_2$ also existed in the solution under special conditions as a less stable terminal-binding species. In Jiang's report using NMR and EXAFS[10], 1,7-coordination mode was confirmed undoubtedly for $UO_2L_2$ complexes. Moreover, 2:2 dimeric complex, though unusually detected, was found in a double-tridentate geometry. No terminal-binding species was found. Kirishima and co-workers[11] investigated the thermodynamic properties of U(VI) complexes with ODA and its corresponding aliphatic/aromatic parallels, and promoted that the complexation of aliphatic ligands were completely entropy driven, while enthalpy and entropy co-influence the progress of the reactions.

As analogues for ODA, the coordination of IDA and TDA with U(VI) were also investigated, and comparisons with ODA were made. The U(VI) complexation properties for IDA are quite similar with those for ODA, including configurations and bond lengths, however, the less positive $\Delta H$ and more positive $\Delta S$ in U(VI)/IDA complexes suggested a greater covalency in U-N bond than $C\text{-}O_{ether}$ in U(VI)/ODA complexes. For TDA, the bridging S is much larger and softer than O and N. However, Bernardo et al.[12] did not find any U/S interactions, who suggested that only the carboxyl groups participated in the coordination. He also held that there was a coordination mode in which TDA formed terminal complexation with uranium.

As described above, several studies focusing on complexation between U(VI) and XDA ligands have been performed. Some structural and thermodynamic data were also obtained, mainly for 1:1 and 1:2 tridentate complexes. From the results, significant differences of U(VI) complexes with the three ligands are observably concluded (i.e. U(VI) complexes with ODA and IDA are similar, but quite different with TDA, also U-O and U-N interactions have been speculated from the atomic distances, but U-S interactions have never been found). However, some questions are still unsolved. Differences between U(VI) complexes are observed, but we still do not know the reasons for those phenomena. U-N bond has been confirmed and $U\text{-}O_{ether}$ bond has been speculated, but whether there are interactions between U and S is still undiscovered. Complex species is strongly dependent on solution conditions (i.e. concentrations and acidity), while only a few species have been proposed. Some unreported species might also co-exist in solution. Furthermore, precise structures could not be obtained via EXAFS measurements due to its unnegligible deviations. Therefore, it is necessary to make a deep investigation on U(VI)/XDA complexes.

Quantum chemistry is a valuable tool that is often used to complement the determined stoichiometric and structural data in order to distinguish among plausible structures and to support the information obtained by spectroscopic means, notably by EXAFS spectroscopy. There has been wealth of experimental and theoretical data in actinide complexes with ODA and its derivatives[11, 13]. It should be mentioned that Wang's group[7] investigated the complexation of Np(V) with ODA, DMOGA and TMOGA through DFT, and found that tridentate structures were more stable than bidentate ones and the substitution of the amide group by carboxylate favors the formation of the complexes. Moreover, he pointed out that Np-$O_{yl}$ bond strength was weakened by coordination.

In the present study, we have been concentrated on the complexation of U(VI) with ODA, IDA and TDA, and made full investigations on the geometries, complexation energies, molecular orbitals and bonding nature. Full comparisons between DFT calculations and experimental data have been made. The results can further improve the understanding of U(VI)/XDA complexation behavior as well as the binding nature between U and different ligand atoms.

## 2. Computational details

In the current study all of the quantum chemistry calculations were carried out with density functional theory (DFT) method with Gaussian09 program[14], which have evolved as a practical and effective computational tool in quantum chemistry[15], especially for large actinide compounds[16, 17]. Calculations were performed with the B3LYP functional, a hybrid Hartree-Fock/DFT method that incorporates Becke's three-parameter functional (B3) with the Lee, Yang, and Parr correlation functional[18, 19]. Stuttgart relativistic small core potential ECP60MWB and the valence basis sets ECP60MWB-SEG augmented with two f-type and two g-type polarization functions were employed[20]. For light atoms (C/H/O/N/S), 6-31G(d) were used in geometry optimizations, and 6-311G(d,p) was employed in other calculations (thermodynamic data, molecular orbitals and AIM analysis). We ensure that all the optimized geometries have no imaginary frequency. The influence of the solvent (water) was modeled using the SMD continuum solvation method[21], where the solute is immersed in a shape adapted isotropic polarizable continuum, with a dielectric constant ε=78.3553 for water. AIM analysis were done based on the atoms-in-molecules (AIM) theory, as implemented in the Multiwfn code[22].

## 3. Results and Discussion

### 3.1 Reliability of theoretical methods

First, we considered the geometry optimization of uranyl aquo ion both in gas and aqueous phases to check the reliability of different methods. Several functionals have been proved to be successful in actinide coordination calculations, including B3LYP[7, 23, 24], MP2[25], BP86[26], etc. Herein, we tested three typical ones of them (B3LYP, MP2 and BP86) using uranyl penta-hydrate as the standard structure ($UO_2(H_2O)_5^{2+}$, shown in Fig. 2).

The obtained values are summarized in Table 1. Data that most close to EXAFS results are computed through B3LYP functional (1.768Å and 2.484Å for U-$O_{yl}$ and U-$OH_2$, respectively in the uranyl ion), which are a little longer (0.002Å and 0.064Å) than the EXAFS results. According to previous theoretical investigations, this deviation is within our acceptable limits. Therefore, B3LYP functional was adopted for all the calculations below.

### 3.2 Structural properties of several U(VI)/XDA binding complexes

Two binding motifs between U(VI) and XDA in the equatorial plane are shown in Fig. 3. Studies have shown that the tridentate mode is prevailing due to the chelating complexation. The terminal-bidentate mode of U(VI)/O=C forming a tetra-membered ring has been proved to be stable in some other studies on uranyl complexes[32, 33]. Hence this mode is also considered here. For 1:2 stoichiometry complexes, the combination of the two motifs results in three possible modes, expressed as tri-/tri, tri-/bi- and bi-/bi- respectively.

Tsushima[34] made an assumption that for uranyl complexes the coordination number (CN) is fixed to five when saturated with water molecules. When the equatorial plane is saturated by other ligands, CN might be four or six. In the present study, complexes of CN four, five and six were all taken into account.

According to the two motifs, we have designed several geometries of the U(VI)/XDA complexes, and the full optimized structures are listed in Fig. 4 with the data in Table 2. From our calculations of 1:1 complexes, it is found that the whole ligands are almost in the equatorial plane of uranyl for ODA, but molecular deformation occurs for IDA and TDA. The U-$O_{yl}$ bond length increases with the binding strength of the complex[34, 35], thus it is reasonable to compare the binding abilities from U-$O_{yl}$ bond lengths. Longer U-$O_{yl}$ bonds (1.784-1.789Å) in tridentate complexes are observed comparing to those in bidentate ones (1.771-1.772Å), suggesting a stronger interaction in the tridentate complexes. This is in line with previous EXAFS and NMR studies[10, 36]. In fact, tridentate complex structures with three water ligands were also calculated. However, in $UO_2(XDA)(H_2O)_3$ geometries, one water ligand lies far away from uranium (~4Å), and we believe it belongs to an outer coordination shell (see Fig. S1). Calculated U-$O_{yl}$ bond lengths (1.77-1.80Å) are exactly the same as in the EXAFS experiments (1.77-1.79Å). The calculations/EXAFS results have shown that U-O(=C) bond lengths are 2.35Å/2.38Å, 2.35Å/2.41Å, 2.41Å/2.40Å, 2.42Å/2.38Å and 2.34Å/2.34Å for O-tri-11, N-tri-11, S-bi-11, O-tri-12 and S-tri/bi-12 complexes, respectively[10]. The deviations of DFT calculations range from 1% to 3%. In strongly acidic solutions, U-X is not formed for both ODA and IDA, proved by the fact of 2.91Å U-$O_{ether}$ bond and 2.92Å U-N bond[10], and this is due to the protonation of bridging atoms (see Fig. S2). The bridging X forms an X--H bond with the solvent, which inhibits the U-X bond formation. In mild acidic solutions (pH>3), the U-X bonds were formed and EXAFS[10]/DFT show bond lengths of 2.50Å/2.57Å and 2.54Å/2.60Å for ODA and IDA respectively. The calculation deviations here are 2.7% and 2.3% respectively. The U-S distance is

3.025Å in our calculations, and to our knowledge, there is no experimental data for U-S bond length up to now.

For complexes of 1:2 stoichiometry, molecular deformation occurred for all the ligands due to over-crowdness, indicating that a steric hindrance takes effect. There is a slight increase in the U-$O_{yl}$ bonds comparing to 1:1 complexes, and the U-X bonds are largely elongated. The double tridentate structures have the largest U-$O_{yl}$ bonds, indicating more stable than others. It is quite surprising that in this structure of U(VI)/TDA, one S atom leaves far away from U (4.61Å), indicating no interactions between them. In S-tri/bi-12 complex where two TDA ligands take the tridentate and bidentate modes at the same time, the calculation/EXAFS results are nearly identical, 2.34Å/2.34Å and 2.50Å/2.49Å for U-O(=C) bonds in tridentate and bidentate ligands respectively[12]. 1:2 double bidentate species for all U/XDA complexes have not been reported.

Optimizations of 2:2 complexes were also calculated, as detected via EXAFS by Jiang et al.[10]. He suggested that 2:2 species is in equilibrium with 1:1 species at higher pH, though never dominant because of the onset of precipitation. In this structure, each uranium is surrounded by five coordination atoms, three with XDA and two with $OH^-$. As the binding ability of $OH^-$ is much stronger than that of $H_2O$, confirming by the fact that U-O(H) (2.38~2.39Å) has a shorter bond length than U-O($H_2$), the U-$O_{yl}$ bond is slightly elongated. The U-U distance is 3.84/3.86/3.85Å for ODA/IDA/TDA respectively, shorter than the EXAFS results in aqueous solutions[10] (ODA 4.31Å; IDA 4.33Å), but quite close to the X-ray crystallographic data[36] (ODA 3.76Å; IDA 3.85Å). There has been no EXAFS data for 2:2 complex structure of U(VI)/TDA dimer yet.

In general, 1:1 tridentate and 1:2-tridentate complexes were calculated through DFT, which were investigated by previous EXAFS studies. And the data between them have shown the accuracy of our calculations. We also predicted some species that have not been reported, especially which contain bidentate ligands. Calculation results show that coordination bonds are formed between U and O(=C), the bridging X atoms, O($H_2$) and O($H^-$). The bond length, which is indicative of bond strength, is in the sequence: U-O(=C) > U-O($H^-$) > U-O($H_2$) > U-X. CN five is mostly observed for these complexes, while CN four and six are also found here.

### 3.3 Complexation stability

To investigate the nature of complexation reactions and stability of complexes, we carried out the energy calculations. Table 3 lists the changes in complexation energies for complexation reactions between aquo uranyl ion and the three ligands in aqueous solutions as well as the stability constants reported by previous studies. The initial species of U(VI) in the reactions was the aquo uranyl ion (penta-hydrate). The enthalpy and entropy trends of available experimental data are displayed in Fig. S4 and Table S1.

As presented in Table 3, the gas phase complexation energies are mostly from -469.3 to -127.3 kcal/mol, and the hydration complexation energies range from -89.2 to -17.7 kcal/mol. It can be clearly seen that all the reactions energies are negative, suggesting spontaneous complexation processes. However, the complexation energies in gas phase are one order of magnitude more negative than those in hydration phase. This means that there is a quite strong interaction between U(VI) and the three ligands inherently, while in aqueous phase the charges and polarities are partially shielded which reduces the interaction.

For 1:1 complexes, the tridentate ones are obviously more stable than the bidentate ones due to the chelating effect. The complexation energy of U(VI)/IDA is a slight more negative than U(VI)/ODA. For terminal bidentate complexes, the complexes with three and two water ligands were both taken into account, and the reaction energy calculations imply that the ones with three water ligands are less stable than the ones with two water ligands by only 2-4 kcal/mol differences. Bernardo et al.[12] held that there were three water ligands participating in the terminal bidentate structure of U(VI)/TDA complex with an average U-$O_{eq}$ bond length 2.40Å. This fact seems to be a little different with our calculations. However in our opinion, such a small energy barrier (2~4 kcal/mol) between the two structures is so insignificant that possible transformation to each other might occur depending on the solution conditions. U(VI) bidentate complexes with ODA and IDA have not been reported till now. Possibly the differences for U(VI)/ODA or U(VI)/IDA complexes between their tridentate and bidentate modes are much more larger than U(VI)/TDA complex. From complexation energies, the tridentate complexes are 12-23 kcal/mol more stable than bidentate ones. Moreover, the complexation stability for U(VI) with three XDA ligands is as follow: IDA > ODA >> TDA, which agrees well with the log$\beta$ data.

For 1:2 complexes, three geometries (including double tridentate, combining tridentate and bidentate, double bidentate, which are briefly named 'tri-','tri-/bi-' and 'bi-' in the tables respectively) were considered. It is shown from Table 3 that the double tridentate structures have rather negative complexation energies, in which case the CN of uranium is six for ODA and IDA, but five for TDA (one sulfur atom has no interaction with uranium as discussed above). The substitution of one bidentate ligand for one tridentate ligand would bring about an energy rise from 3 to 20 kcal/mol. It should be mentioned that in the double bidentate structures, the cases with one, two and no water ligands were taken into account, and the complexes without water ligands were found the most stable (the complexation energy is 1~4 kcal/mol and 5~7 kcal/mol more negative than those for complexes with one and two water ligands respectively). In the case, the CN of uranium is four. We have established three binding modes for 1:2 complexes, however, the double bidentate ones have not been found by experimental studies. From the complexation energies this species is less stable. The 'tri-/bi-' ones are also seldom reported, with exception of U(VI)/TDA complexes. The double tridentate ones have been reported in detail, including both structures and thermodynamics. Also, complexation stability is in the sequence IDA > ODA >> TDA for both calculation and experimental results.

According to discussions above, it is easily observed that the tridentate mode makes a much larger contribution to the stability of the complexes. Thus, in 2:2 complexes we only took the double tridentate mode into account. From Table 3 it is shown that the double tridentate complexes are the most stable ones for ODA, IDA and TDA, suggesting a high thermodynamic stability. For 2:2 species, all the complexes have the most negative reaction energies, indicating the considerable stability of the species. Large decline of enthalpy change after the participation of hydroxyl ions brings about an increase in stability. Nevertheless, this species could not be easily detected due to low solubility. Jiang et al.[10] reported this 2:2 complexes for both ODA and IDA, but the corresponding TDA complex was not found. The large stability constants are in accordance with our calculations.

As is seen from Table 3, experimental thermodynamic data for all of the 1:1 and 1:2 tridentate complexes have been determined, but for other modes not. In each tridentate mode, the complexation stabilities for both theoretical calculations and experiments have the same trend IDA > ODA >> TDA. But it seems that the complexation stabilities for U(VI)/ODA complexes are overestimated comparing to the stability constants. Jiang et al.[10] found a ~20ppm downfield of chemical shifts through $^{15}N$ NMR, and suggested the formation of U-N coordination bond. However, in $^{13}C$ NMR results, he found no observable change of chemical shifts occurred under the experimental conditions. He speculated that the fast breaking and reforming of the U-$O_{ether}$ bond took place. Choppin et al.[38] suggested that the U-$O_{ether}$ bond could be relatively more labile than the U-N bond and therefore a stronger interaction of U-N for IDA may occur than U-$O_{ether}$ for ODA. To confirm it, we performed the scanning of potential energy surface (PES) for U(VI)/ODA tridentate complexes (O-tri-11) in aqueous solutions (see Fig. S3). The U-X bond length was changed from 2.50Å to 2.74Å by a 0.01Å step. From the tendency of the single point energies ($E_{sp}$), it is observed that there are two local minima where the U-$O_{ether}$ bond lengths are 2.57Å and 2.68Å respectively. The variation of the energy during the scanning is rather smooth, indicating that the dynamic process for U-$O_{ether}$ bond quite possibly occurs. This makes the reaction Gibbs free energy less negative to some degree, and is possibly responsible for the overestimation of complexation stability for U(VI)/ODA.

Comparing DFT calculations and experimental data, a much stronger preference for tridentate chelation has been found. For the three ligands, the complexation stabilities are in the sequence IDA > ODA >> TDA in each binding mode, in line with the experimental data. The breaking-reforming dynamic process of U-$O_{ether}$ bond possibly exists.

### 3.4 MO and AIM analysis

Molecular orbital (MO) analysis was carried out to investigated the interactions between U(VI) and XDA ligands, and some occupied MOs are displayed in Fig. 5. It is observed that the relatively diffuse 5f orbitals mainly participate in the bondings for the complexes, with 6p and 6d orbitals playing minor roles. The occupied MOs correspond to U-O(=C) and U-X σ bonds, resulting from the contributions of U-5f orbital and p orbitals of ligand atoms. Fig. 5b-e clearly indicate that the interactions of U and X atoms are considerable. It should be noted that the electronic interaction of U-S bond is observable, which has not been reported for U(VI)/TDA complexes.

To further understand the bonding nature of U(VI)/XDA complexes, Atoms-In-Molecule (AIM) topological analysis has been employed. AIM analysis is often applied in the study of nature of chemical bonds, which was promoted by Bader[39]. Numerous examples have demonstrated the accuracy and practicality of this method[40, 41], including in actinide chemistry[42-44]. Instead of orbital structures, AIM analysis is concentrated on the molecular electron density. Based on AIM theory, there is one bond critical point (BCP) between each pair of atoms that are bonded to each other, being the saddle point on the electron density curve, a minimum in one direction and a maximum in its perpendicular direction. BCP is related to the minimum electron density for an electron pair. The electron density contour maps of the three 1:1 tridentate complexes are displayed in Fig. 6. Values of two important indicators are marked in the figures, the electron density $\rho(r)$ and the Laplacian of electron density $\nabla^2\rho(r)$ respectively, which are often used to predict the bonding properties. According to Bader's theory, a covalent bond has a negative $\nabla^2\rho(r)$ and a $\rho(r)$ above 0.2 a.u.; also, an ionic bond has a positive $\nabla^2\rho(r)$ and a $\rho(r)$ lower than 0.1 a.u. Therefore, all the U-O(=C) and U-X coordination bonds are typically ionic bonds.

In general, the magnitude of electron density is an indicator of the strength of a chemical bond. As seen in Fig. 6, the electron density ranges from 0.072 a.u. to 0.074 a.u., suggesting the U-O(=C) bonds have similar bonding strengths for all the complexes. On the contrary, the electron density values are more different for U-X bonds, following the order U-N > U-O > U-S which is in the same sequence of complexation stability. Therefore, we consider that the strength of U-X bonds is mainly responsible for the differences of U(VI)/XDA complexes. Comparing to U-O(H2) bonds, there is a larger accumulation of electron density along the U-O(=C) bonds, indicating a much stronger interaction of the U-O(=C) bonds, which is in the same trend of bond lengths. In a word, the magnitude of electron density and the bonding strength for all the coordination bonds are in the sequence U-O(=C) > U-N > U-O($H_2$) ≈ U-$O_{ether}$ > U-S.

## 4. Conclusions

Theoretical calculations have been carried out to investigate the complexation of uranium with ODA, IDA and TDA. The present results contribute to a better understanding of the coordination of uranium to these ligands. From the structural information, complexation stability and topological analysis, the main conclusions are summarized as follows.

(1) The binding ability of groups or atoms in ligands is in the order: >C=O > $OH^-$>> $H_2O$ >X. The coordination number five is most common, while four and six are also observed in our calculations. The steric hindrance of molecules plays a significant role in 1:2 complexes, especially for U(VI)/TDA complexes.

(2) The stability of uranyl complexes is in the order IDA>ODA>>TDA from the aspect of ligand types, 2:2 > 1:2 > 1:1 from the aspect of stoichiometries, and tridentate > bidentate from the aspect of binding modes. The participation of $OH^-$ ion stabilizes 2:2 complexes to a large extent.

(3) The diffuse 5f-orbital of U and p-orbitals of O/N/S contribute to the coordination bonds. All of the coordination bonds are typically ionic. U-O(=C) bonds play a dominant role on complexation, while U-X bonds also take an unnegligible effect. The strength of U-X bonds follows the U-N > U-$O_{ether}$ > U-S, same with complexation stability sequence. The interaction of U and S is found via electron density analysis, which has not been reported by neither experiments nor theoretical

studies before.

## Acknowledgement

This work was supported by National Natural Science Foundation of China (21507118 &21303068). We are really appreciated for the help from Prof. Dongqi Wang (Institute of High Energy Physics Academy of Sciences) and Prof. Yongfan Zhang (Fuzhou University).

## References

1. P. L. Zanonato, P. Di Bernardo and I. Grenthe, *Dalton Transactions*, 2014, **43**, 2378-2383.
2. Z. Zhang, G. Helms, S. B. Clark, G. Tian, P. Zanonato and L. Rao, *Inorganic Chemistry*, 2009, **48**, 3814-3824.
3. M. Sun, L. Yuan, N. Tan, Y. Zhao, Z. Chai and W. Shi, *Radiochimica Acta*, 2014, **102**, 87-92.
4. Y. Zhang, I. Karatchevtseva, M. Bhadbhade, T. T. Tran, I. Aharonovich, D. J. Fanna, N. D. Shepherd, K. Lu, F. Li and G. R. Lumpkin, *Journal of Solid State Chemistry*, 2016, **234**, 22-28.
5. G. Tian, L. Rao, S. J. Teat and G. Liu, *Chemistry-a European Journal*, 2009, **15**, 4172-4181.
6. R. Linfeng and T. Guoxin, *Actinides 2005-Basic Science, Applications and Technology. Symposium (Materials Research Society Symposium Proceedings)*, 2006, **893**, 305-314.
7. J. Zeng, X. Yang, J. Liao, N. Liu, Y. Yang, Z. Chai and D. Wang, *Physical Chemistry Chemical Physics*, 2014, **16**, 16536-16546.
8. J. I. Friese, K. L. Nash, M. P. Jensen and J. C. Sullivan, *Radiochimica Acta*, 1998, **83**, 175-181.
9. L. Rao, A. Y. Garnov, J. Jiang, P. Di Bernardo, P. Zanonato and A. Bismondo,

*Inorganic Chemistry*, 2003, **42**, 3685-3692.

10. J. Jiang, J. C. Renshaw, M. J. Sarsfield, F. R. Livens, D. Collison, J. M. Charnock and H. Eccles, *Inorganic Chemistry*, 2003, **42**, 1233-1240.

11. A. Kirishima and N. Sato, *Journal of Chemical Thermodynamics*, 2014, **70**, 227-232.

12. P. Di Bernardo, P. Zanonato, A. Bismondo, H. Jiang, A. Y. Garnov, J. Jiang and L. Rao, *European Journal of Inorganic Chemistry*, 2006, DOI: 10.1002/ejic.200600554, 4533-4540.

13. R. Linfeng and T. Guoxin, *Complexation of actinides with amide derivatives of oxydiacetic acid*, 2006.

14. M. Frisch, G. Trucks, H. Schlegel, G. Scuseria, M. Robb, J. Cheeseman, G. Scalmani, V. Barone, B. Mennucci and G. Petersson, *Gaussian Inc., Wallingford, CT*, 2009, **270**, 271.

15. D. Shen, C. Kong, R. Jia, P. Fu and H. Zhang, *Journal of Physical Chemistry A*, 2015, **119**, 3636-3643.

16. Y. Wang, L. Song, L. Zhu, B. Guo, S. Chen and W. Wu, *Dalton Transactions*, 2014, **43**, 3739-3749.

17. H. Hu, F. Wei, X. Wang, L. Andrews and J. Li, *Journal of the American Chemical Society*, 2014, **136**, 1427-1437.

18. A. D. Becke, *Physical Review A*, 1988, **38**, 3098-3100.

19. C. Lee, W. Yang and R. G. Parr, *Physical Review B*, 1988, **37**, 785-789.

20. X. Cao, M. Dolg and H. Stoll, *The Journal of Chemical Physics*, 2003, **118**, 487-496.

21. A. V. Marenich, C. J. Cramer and D. G. Truhlar, *The Journal of Physical Chemistry B*, 2009, **113**, 4538-4543.

22. T. Lu and F. Chen, *Journal of Computational Chemistry*, 2012, **33**, 580-592.

23. D. Das, E. V. Goud, S. Annam, S. Jayalakshmi, G. Gopakumar, C. V. S. B. Rao, N. Sivaraman, A. Sivaramakrishna and K. Vijayakrishna, *RSC Advances*, 2015, **5**, 107421-107429.

24. C. Wang, J. Lan, Q. Wu, Q. Luo, Y. Zhao, X. Wang, Z. Chai and W. Shi,

*Inorganic Chemistry*, 2014, **53**, 9466-9476.

25. H. Moll, A. Rossberg, R. Steudtner, B. Drobot, K. Mueller and S. Tsushima, *Inorganic Chemistry*, 2014, **53**, 1585-1593.
26. Q. Wu, C. Wang, J. Lan, C. Xiao, X. Wang, Y. Zhao, Z. Chai and W. Shi, *Inorganic Chemistry*, 2014, **53**, 9607-9614.
27. X. Wang, G. Zhu and F. Guo, *Annals of Nuclear Energy*, 2013, **56**, 151-157.
28. C. Xu, J. Su, X. Xu and J. Li, *Sci. China Chem.*, 2013, **56**, 1525-1532.
29. X. Guo, Y. Wang, C. Li, P. Huai and G. Wu, *Molecular Physics*, 2015, **In press**.
30. J. Neuefeind, L. Soderholm and S. Skanthakumar, *The Journal of Physical Chemistry A*, 2004, **108**, 2733-2739.
31. M. Aaberg, D. Ferri, J. Glaser and I. Grenthe, *Inorganic Chemistry*, 1983, **22**, 3986-3989.
32. C. Lucks, A. Rossberg, S. Tsushima, H. Foerstendorf, A. C. Scheinost and G. Bernhard, *Inorganic Chemistry*, 2012, **51**, 12288-12300.
33. C. Z. Wang, J. H. Lan, Q. Y. Wu, Q. Luo, Y. L. Zhao, X. K. Wang, Z. F. Chai and W. Q. Shi, *Inorganic Chemistry*, 2014, **53**, 9466-9476.
34. S. Tsushima, *Dalton Transactions*, 2011, **40**, 6732-6737.
35. C. Kong, E. A. J. F. Peters, Q. Zheng and H. Zhang, *Physical Chemistry Chemical Physics*, 2014, **16**, 9634-9642.
36. J. Jiang, M. J. Sarsfield, J. C. Renshaw, F. R. Livens, D. Collison, J. M. Charnock, M. Helliwell and H. Eccles, *Inorganic Chemistry*, 2002, **41**, 2799-2806.
37. P. D. Bernardo, G. Tomat, A. Bismondo, O. Traverso and L. Magon, *Journal of Chemical Research (Miniprint)*, 1980, 3044-3071.
38. G. R. Choppin, L. F. Rao, E. N. Rizkalla and J. C. Sullivan, *Journal*, 1992, **57**, 173.
39. R. F. W. Bader, *The Journal of Physical Chemistry A*, 1998, **102**, 7314-7323.
40. R. N. Behera and A. Panda, *RSC Advances*, 2012, **2**, 6948-6956.
41. K. Srivastava, M. R. Shimpi, A. Srivastava, P. Tandon, K. Sinha and S. P.

Velaga, *RSC Advances*, 2016, **6**, 10024-10037.

42. P. Li, W. Niu and T. Gao, *RSC Advances*, 2014, **4**, 29806-29817.

43. C. Xiao, C. Wang, L. Mei, X. Zhang, N. Wall, Y. Zhao, Z. Chai and W. Shi, *Dalton Transactions*, 2015, **44**, 14376-14387.

44. E. Hashem, A. N. Swinburne, C. Schulzke, R. C. Evans, J. A. Platts, A. Kerridge, L. S. Natrajan and R. J. Baker, *RSC Advances*, 2013, **3**, 4350-4361.

**Table 1. Average bond lengths (in Å) and angles (in deg.) of $UO_2(H_2O)_5^{2+}$ in the present and previous studies**

| Phase | | Methods | U=O | U-OH$_2$ | ∠(O=U=O) |
|---|---|---|---|---|---|
| gas | this paper | B3LYP | 1.748 | 2.481 | 177.936 |
| | | MP2 | 1.771 | 2.487 | 179.658 |
| | | BP86 | 1.772 | 2.465 | 174.704 |
| | elsewhere | B3LYP[25] | 1.749 | 2.496 | 178.160 |
| | | B3LYP[27] | 1.753 | 2.539 | -- |
| | | BP86[27] | 1.775 | 2.472 | -- |
| aqueous | this paper | B3LYP | 1.768 | 2.484 | 179.619 |
| | | MP2 | 1.772 | 2.460 | 179.738 |
| | | BP86 | 1.771 | 2.461 | 175.001 |
| | elsewhere | B3LYP[28] | 1.75 | 2.43-2.51 | -- |
| | | B3LYP[29] | 1.762 | 2.465 | 178.845 |
| | | EXAFS[30] | 1.766 | 2.420 | -- |
| | | X-ray Scattering[31] | 1.702 | 2.421 | -- |

**Table 2. Bond lengths of U(VI)/XDA complexes in aqueous solutions (in Å)**

| Mode | U-O$_{yl}$ | U-O(H$_2$) | U-O(=C) | U-O$_{ether}$ | U-N | U-S |
|---|---|---|---|---|---|---|
| O-tri-11 | 1.784 | 2.540, 2.542 | 2.337-2.349 | 2.565 | -- | -- |
| N-tri-11 | 1.789 | 2.341, 2.571 | 2.341-2.345 | -- | 2.598 | -- |
| S-tri-11 | 1.784 | 2.544, 2.566 | 2.329-2.336 | -- | -- | 3.025 |
| O-bi-11 | 1.771 | 2.479, 2.486 | 2.427-2.464 | 5.025 | -- | -- |
| N-bi-11 | 1.772 | 2.464, 2.480 | 2.430-2.449 | -- | 5.083 | -- |
| S-bi-11 | 1.771 | 2.480, 2.485 | 2.411-2.475 | -- | -- | 5.328 |
| O-tri-12 | 1.792 | -- | 2.421-2.439 | 2.716, 2.771 | -- | -- |
| N-tri-12 | 1.800 | -- | 2.498-2.530 | -- | 2.672, 2.677 | |
| S-tri-12 | 1.796 | -- | 2.356-2.374 | -- | -- | 3.109, 4.611 |
| O-tri/bi-12 | 1.790 | -- | 2.337-2.520 | 2.571 | -- | -- |
| N-tri/bi-12 | 1.794 | -- | 2.341-2.516 | -- | 2.614 | -- |
| S-tri/bi-12 | 1.789 | -- | 2.335-2.521 | -- | -- | 3.029 |
| O-bi-12 | 1.776 | -- | 2.461-2.468 | -- | -- | -- |
| N-bi-12 | 1.777 | -- | 2.439-2.498 | -- | -- | -- |
| S-bi-12 | 1.776 | -- | 2.449-2.472 | -- | -- | -- |
| O-tri-22 | 1.800 | -- | 2.379-2.381 | 2.577, 2.592 | -- | -- |
| N-tri-22 | 1.803 | -- | 2.375-2.379 | -- | 2.672×2 | -- |
| S-tri-22 | 1.799 | -- | 2.364-2.375 | -- | -- | 3.143, 3.082 |

**Table 3. Complexation energies of various U(VI)/XDA complexes (in kcal/mol)**

| Mode | Reaction | $G_{gas}$ | $G_{aq}$ | log$\beta$ |
|---|---|---|---|---|
| O-tri-11 | $UO_2(H_2O)_5^{2+}+ODA^{2-}$—$UO_2ODA(H_2O)_2+3H_2O$ | -392.8 | -40.1 | 5.11[37],<br>5.77[10],<br>5.26[11] |
| N-tri-11 | $UO_2(H_2O)_5^{2+}+IDA^{2-}$—$UO_2IDA(H_2O)_2+3H_2O$ | -390.0 | -41.9 | 9.90[10] |
| S-tri-11 | $UO_2(H_2O)_5^{2+}+TDA^{2-}$—$UO_2TDA(H_2O)_2+3H_2O$ | -182.2 | -29.6 | 2.79[11] |
| O-bi-11 | $UO_2(H_2O)_5^{2+}+ODA^{-}$—$UO_2ODA(H_2O)_2^{+}+3H_2O$ | -196.8 | -18.5 | -- |
| N-bi-11 | $UO_2(H_2O)_5^{2+}+IDA^{-}$—$UO_2IDA(H_2O)_2^{+}+3H_2O$ | -198.5 | -18.7 | -- |
| S-bi-11 | $UO_2(H_2O)_5^{2+}+TDA^{-}$—$UO_2TDA(H_2O)_2^{+}+3H_2O$ | -127.3 | -17.7 | 5.76[12],<br>5.43[37] |
| O-tri-12 | $UO_2(H_2O)_5^{2+}+2ODA^{2-}$—$UO_2(ODA)_2^{2-}+5H_2O$ | -469.3 | -59.5 | 7.84[11] |
| N-tri-12 | $UO_2(H_2O)_5^{2+}+2IDA^{2-}$—$UO_2(IDA)_2^{2-}+5H_2O$ | -457.6 | -59.9 | 16.42[10] |
| S-tri-12 | $UO_2(H_2O)_5^{2+}+2TDA^{2-}$—$UO_2(TDA)_2^{2-}+5H_2O$ | -62.5 | -51.0 | 1.76[11] |
| O-tri/bi-12 | $UO_2(H_2O)_5^{2+}+ODA^{-}+ODA^{2-}$—$UO_2(ODA)_2^{-}+5H_2O$ | -309.5 | -51.4 | -- |
| N-tri/bi-12 | $UO_2(H_2O)_5^{2+}+IDA^{-}+ODA^{2-}$—$UO_2(IDA)_2^{-}+5H_2O$ | -431.5 | -55.6 | -- |
| S-tri/bi-12 | $UO_2(H_2O)_5^{2+}+TDA^{-}+ODA^{2-}$—$UO_2(TDA)_2^{-}+5H_2O$ | -149.0 | -42.5 | 8.48[12],<br>8.39[37] |
| O-bi-12 | $UO_2(H_2O)_5^{2+}+2ODA^{-}$—$UO_2(ODA)_2+5H_2O$ | -310.6 | -31.0 | -- |
| N-bi-12 | $UO_2(H_2O)_5^{2+}+2IDA^{-}$—$UO_2(IDA)_2+5H_2O$ | -300.5 | -32.2 | -- |
| S-bi-12 | $UO_2(H_2O)_5^{2+}+2TDA^{-}$—$UO_2(TDA)_2+5H_2O$ | -157.5 | -29.8 | -- |
| O-tri-22 | $UO_2(H_2O)_5^{2+}+ODA^{2-}+OH^{-}$— $1/2(UO_2)_2(ODA)_2(OH)_2^{2-}+5H_2O$ | -491.9 | -88. 5 | 4.29[10] |
| N-tri-22 | $UO_2(H_2O)_5^{2+}+IDA^{2-}+OH^{-}$— $1/2(UO_2)_2(IDA)_2(OH)_2^{2-}+5H_2O$ | -487.1 | -89.2 | 10.80[10] |
| S-tri-22 | $UO_2(H_2O)_5^{2+}+TDA^{2-}+OH^{-}$— $1/2(UO_2)_2(TDA)_2(OH)_2^{2-}+5H_2O$ | -282.3 | -78.1 | -- |

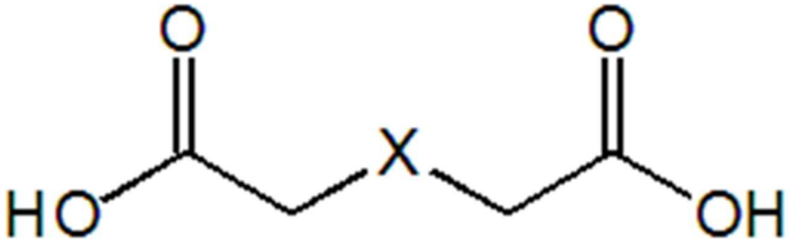

Fig. 1 Scheme for ODA, IDA and TDA where X=O, NH and S respectively

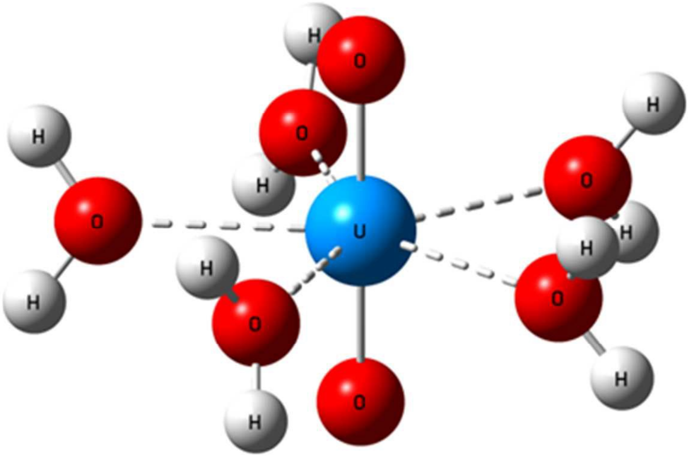

Fig. 2 The optimized structure of $UO_2(H_2O)_5^{2+}$ in aqueous solution using B3LYP functional

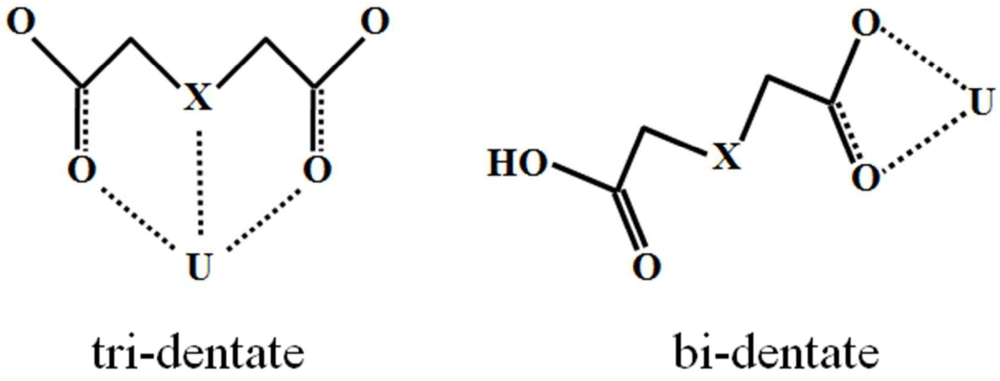

Fig. 3 Binding motifs of uranium and XDA (X=O/NH/S)

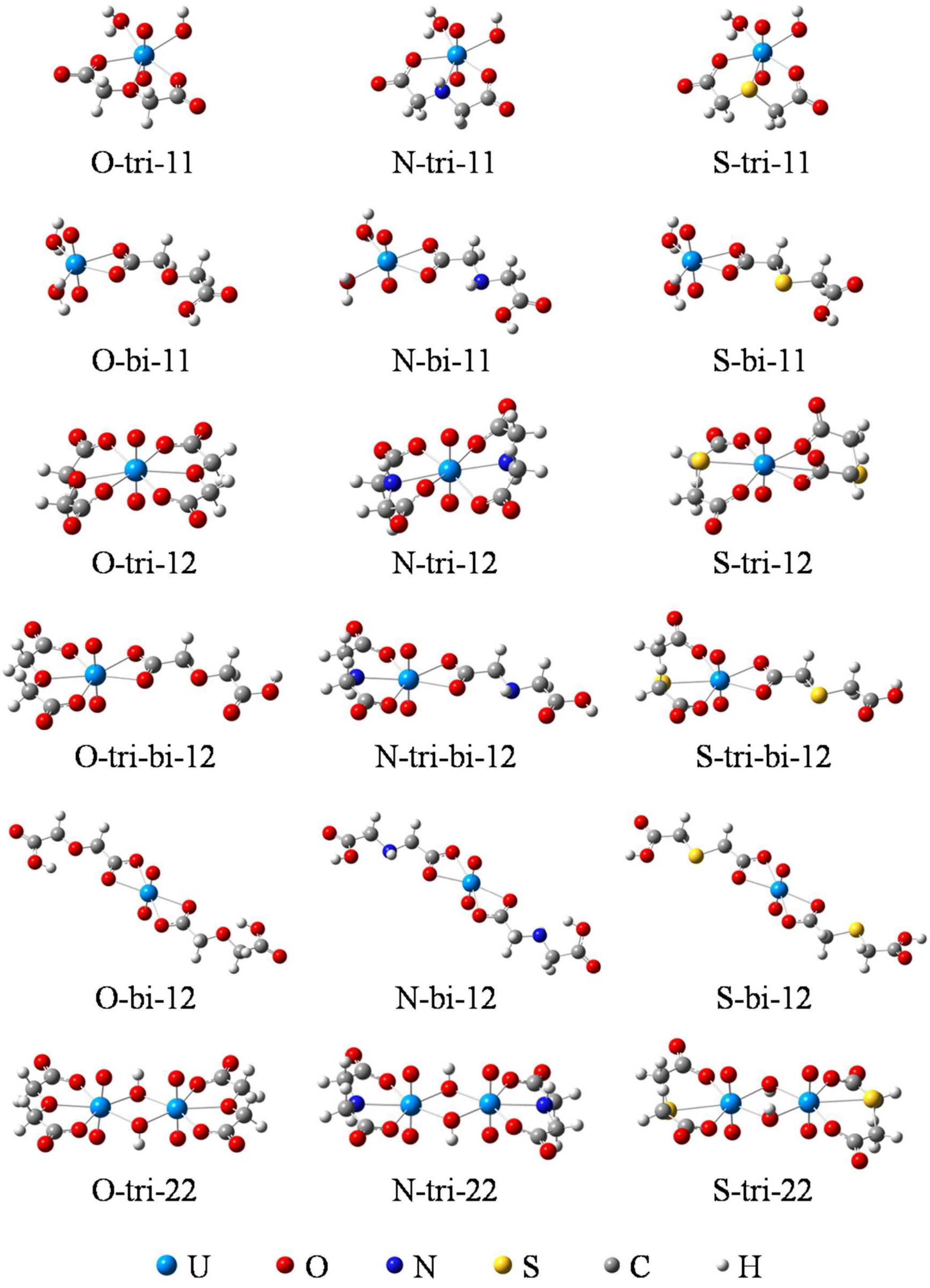
O-tri-11 N-tri-11 S-tri-11

O-bi-11 N-bi-11 S-bi-11

O-tri-12 N-tri-12 S-tri-12

O-tri-bi-12 N-tri-bi-12 S-tri-bi-12

O-bi-12 N-bi-12 S-bi-12

O-tri-22 N-tri-22 S-tri-22

Fig. 4 Full optimized geometries of U(VI)/XDA complexes

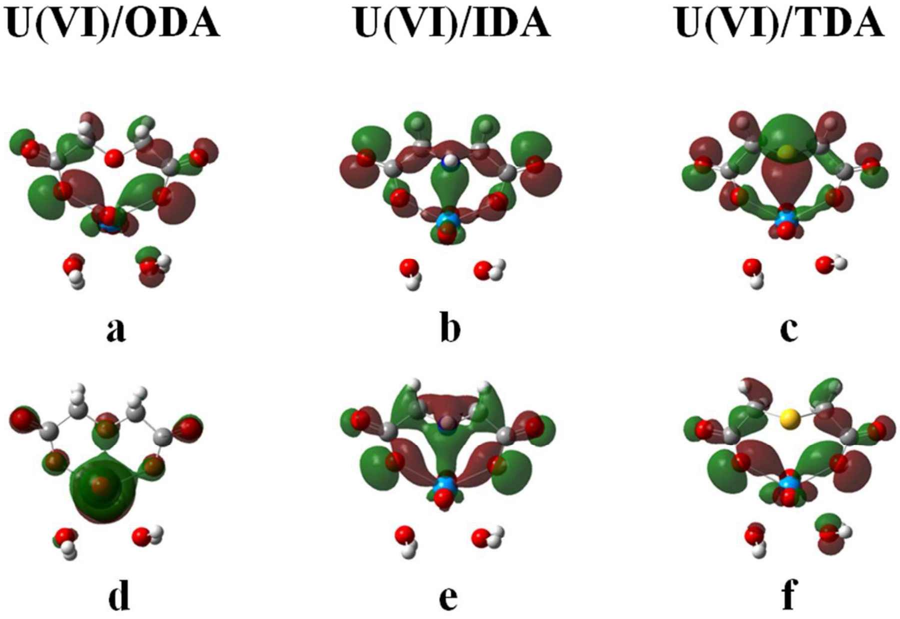

Fig. 5 Some MOs of 1:1 tridentate U(VI)/XDA complexes

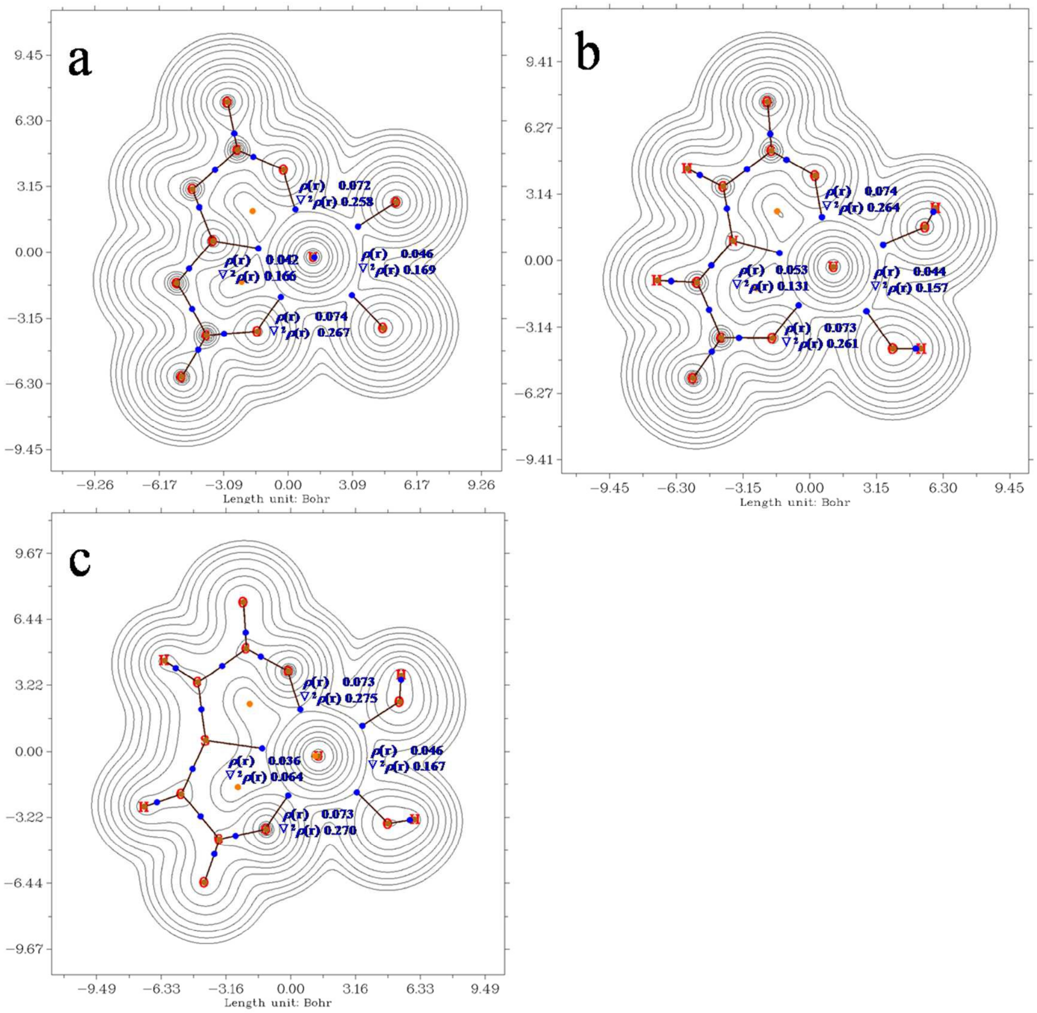

Fig. 6 Electron density contour maps of 1:1 tridentate U(VI)/XDA complexes: ODA(a), IDA(b) and TDA(c)

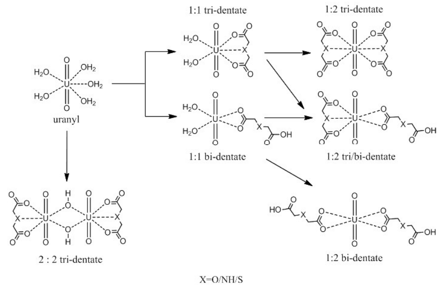

Graphical Abstract

Precise structures of U(VI) complexes with ODA, IDA and TDA in different binding modes.